Sixth International Conference on Durability of Concrete Structures **Paper Number MID01**
18 - 20 July 2018
University of Leeds, Leeds, West Yorkshire, LS2 9JT, United Kingdom

Surface Treatments for Concrete under Physical Salt Attack

M.R. Sakr[1,2] and M.T. Bassuoni[1]
[1]Civil Engineering, University of Manitoba, Winnipeg, Canada
[2]Civil Engineering, Faculty of Engineering at Shoubra, Benha University, Egypt

ABSTRACT

Physical salt attack (PSA) is a key deterioration mechanism for concrete structures in contact with salt-rich media. Yet, procedures and techniques for protecting and repairing concrete affected by PSA are not adequately addressed in the technical literature. Therefore, in this study, three surface coatings of concrete were tested to determine their ability to withstand conditions stimulating to PSA. The treatments were selected to achieve either a single function such as acting as a membrane layer or hydrophobic agent, or combined pore blocking and water repelling functions. Coatings were applied on a concrete mixture typically used for residential foundations in Canada. Mass change was used as a measure to quantify the damage, in addition to microscopy and mineralogical analyses to elucidate the damage mechanisms. The results showed that the damage in deteriorating specimens was due to a combination of physical and chemical sulfate attacks. Also, epoxy and ethyl silicate were effective at protecting concrete from sodium sulfate damage while silane was not.

Keywords: Physical salt attack, Sulfate Attack, Surface treatments, Repair, Durability, Concrete.

1.0 INTRODUCTION

Physical salt attack (PSA) has been recognized as a cause of deterioration of concrete structures under a range of environments that leads to progressive scaling and flaking of concrete surface disrupting its performance (Haynes and Bassuoni, 2011). PSA usually occurs on the evaporative front (exposed to ambient conditions) of elements exposed to salt-rich soils with many field cases such as residential foundations, slab on grades and tunnels (Yoshida *et al.*, 2010; Liu *et al.*, 2017). Moreover, the encountered damage is mainly physical in nature with limited or no chemical alteration of hydration products involved (Folliard and Sandberg, 1994; Haynes *et al.*, 1996; Flatt, 2002). Salt (e.g. sodium sulfate, sodium carbonate, etc.) crystals grow inside a confined pore space exerting crystallization pressure on the pore walls (Haynes *et al.*, 2008). Flatt (2002) reported that the value of pressure can reach 10–20 MPa, which is far greater than the tensile strength of concrete; thus causing its damage.

Historically, PSA was confused with chemical attacks caused by sulfate salts. For instance, in the long-term field study commenced by Portland Cement Association (PCA) on sulfate resistance of concrete specimens partially embedded in sulfate-rich soil, the distress in specimens was first misidentified as chemical sulfate attack (Stark, 1989); however, in 2002, a subsequent report indicated that damage was located only above the ground level with minor damage experienced under this level which was not characteristic of chemical damage. Stark (2002) attributed the cause of damage to PSA; also, it was stated that the physical damage was far more prominent than that resulting from chemical attack.

Although conventional methods to enhance concrete performance (e.g. reducing water-to-binder ratio (w/b) and using supplementary cementitious materials [SCMs] can be successful in protecting concrete from some durability issues, they are not fully applicable to the case of PSA. For example, while reducing w/b can reduce the level of PSA damage, it can still occur even for low w/b (Bassuoni and Rahman, 2016). Also, several studies reported that incorporating SCMs (e.g. fly ash, slag and silica fume) as a partial replacement of ordinary cement leads to escalation of the surface scaling (Nehdi *et al.*, 2014; Zhutovsky and Hooton, 2017). Therefore, research should be directed to develop other efficient techniques regarding this aspect.

One laboratory study attempted to determine the suitability of four surface treatment materials to resist PSA on concrete (Suleiman *et al.*, 2014). Coated cylinders were partially immersed in a 5% Na_2SO_4 solution and subjected to cyclic temperature and RH (one week at 20°C/82% RH followed by one week at 40°C/31% RH) for a duration of six months. Epoxy and silane were reported to be successful in resisting PSA due to their barrier and hydrophobic effect, respectively. The bitumen coating achieved similar protection to epoxy when applied on concrete with w/b of 0.4; however, for concretes with w/b of 0.5, the coating detached as water molecules might

entrap between the bitumen layer and the concrete surface. The acrylic based coating was not adequate in resisting conditions stimulating to PSA. Nevertheless, it should be mentioned that the test conditions applied were not sufficiently severe to conclusively judge the suitability of these coatings as the maximum reported mass loss for uncured uncoated specimens was less than 3%.

2.0 RESEARCH SIGNIFICANCE

Although physical salt attack is a key mechanism of concrete deterioration in salt-rich media, limited research exists on the protection of concrete elements vulnerable to PSA during their service life. Therefore, the aim of this paper was to investigate the potential application of some surface treatments to provide protection against conditions stimulating to PSA. The aggravated test conditions were selected to ensure reasonable conclusions on the applicability of these coatings in field exposures. This research should enhance the existing knowledge on protecting concrete elements vulnerable to PSA

3.0 EXPERIMENTAL PROGRAM

3.1 Materials

Base Mixture

To check the suitability of various surface treatments for concrete to resist PSA, a base concrete mixture with w/b of 0.60 was used to represent the substrate for coatings. The high w/b was chosen to simulate the construction practices in North America for residential concrete. General use cement (GU), which meet CSA A3001 (CAN/CSA-A3001, 2013) specifications was used. Locally available natural gravel (max. size of 9.5 mm) was used as coarse aggregate, with specific gravity and absorption of 2.65 and 2%, respectively. Also, well graded river sand was used as fine aggregate with specific gravity, absorption, and fineness modulus of 2.53, 1.5% and 2.9, respectively. The total cement, sand and gravel contents were 400, 409 and 1200 kg/m^3, respectively. Concrete (denoted as GU0.6) was cast according to ASTM C192 (2016) (Standard Practice for Making and Curing Concrete Test Specimens in the Laboratory) to prepare triplicate cylinders (75×150 mm) for each type of coating. All the specimens were demoulded after 24 h and cured in a standard curing room (maintained at a temperature of 22±2^{o}C and RH of more than 95%) for 28 days.

Coatings

Three kinds of resins performing different functions (epoxy, silane, and ethyl silicate) were employed as protective agents. Epoxy can penetrate the concrete surface and act as a membrane layer when hardened. In this study, bisphenol-A-(epichlorhydrin) resin mixed with solvent naphtha and 2-methylnaphthalene was used as the primary epoxy resin. The curing agent was a mixture of quartz, benzyl alcohol, 2,2,4 (or 2,4,4)-trimethylhexane-1,6-diamine, solvent naphtha, Isophoronediamine, 2,4,6-tris(dimethylaminomethyl)phenol and naphthalene. Silane penetrates into concrete and reacts with water and alkaline species present in concrete, generating an active hydrophobic ingredient on the pore walls to lower the water absorbency of the treated concrete. The typical molecular structure of silane is in the form of R–Si–OR' where R and R' are functional group and methyl (or ethyl), respectively. The first step of reaction between silane and concrete is the former hydrolysis when reacting with water in capillary pores to form unstable silanol groups that will lose water and condensate into silicone resin. Then, silanol groups in the resin react with hydroxyl groups in concrete pores to provide the hydrophobic effect (Woo *et al.*, 2008). Finally, ethyl silicate (or tetraethylorthosilicate, TEOS [$Si(OC_2H_5)_4$]) which has been widely used in stone treatment and conservation is applied. Similar to silane, TEOS is alkoxylsilane compound which hydrolyses into silanol groups after getting contact with alkaline concrete. Silanol groups condensates to form silica gel that leads to a water-repelling effect. Moreover, TEOS reacts with portlandite inside concrete giving calcium silicate hydrate that blocks the pore (i.e. TEOS acts as a pore blocker) (Barberena-Fernández *et al.*, 2015).

3.2 Method of Application

The coatings used were applied as specified by the manufacturers. All concrete surfaces were ensured to be clean, sound and dry (samples were air dried at 20°C and 50% RH for 24 h) to achieve the maximum possible penetration depth. Epoxy comes in two components (resin and hardener) which were pre-stirred separately then, mixed together (1:1 mixing ratio by volume) with a low-speed drill to minimize air entrapment and until uniform colour and consistency were achieved. Two layers were applied to concrete specimens (denoted as GU0.6-EP) using a brush allowing the first layer to set for 24 h and the second one to air cure for three days as specified for chemical exposure. Regarding silane, it was first stirred to ensure the material was fully blended and of uniform consistency. Subsequently, cylinders were sprayed with silane (denoted as GU0.6-S) in three successive layers (time interval of 30 min). Finally, ethyl silicate was applied concrete (denoted as GU0.6-ES) as provided using a low-pressure sprayer. To ensure proper penetration, two cycles of applications were employed such that each cycle consisted of three successive applications at 15 min intervals and the duration between the two cycles was 60 min. All specimens were air cured in laboratory for three days to provide enough time for proper interaction with the substrate concrete. It should be mentioned that coatings were applied

such that 20 mm were left uncoated at the bottom to allow for the ingress of salt solution into concrete which is considered an appropriate approximation for the process of solution ingress in the field.

3.3 Physical Salt Attack (PSA) Exposure and Tests

Following the curing of surface treatments, the initial mass of coated cylinders was determined (using a balance with an accuracy of 0.01 g). Then, specimens were exposed to PSA exposure. Test conditions in this study were selected based on Bassouni and Rahman (2016). This accelerated exposure was found to give reliable conclusion on the resistance of concrete to PSA in a relatively short period of time. One-third of concrete cylinders was partially immersed in high concentration (10 %) sodium sulfate solution. Specimens were placed in plastic containers having a depth of 50 mm and to minimize the evaporation of solution, containers were covered with lids circularly cut to have openings nearly equal (76 mm) to the cylinder diameter. Then, the top part of specimens was subjected to cyclic temperature and humidity conditions to provoke repetitive crystallization between thenardite (Na_2SO_4) and mirabilite ($Na_2SO_4.10H_2O$) (anhydrous and hydrous phases of sodium sulfate, respectively). According to Navarro and Doehne (1999), this conversion results in higher supersaturation ratios that lead to more severe level of damage. The exposure continued for 120 days, where each cycle (24h) consisted of two consecutive stages: 8-hour hot/dry stage (40 ± 2°C and 35 ± 5 % RH) followed by 16-hour temperate/humid stage (20 ± 2 °C and 90 ± 5 % RH). Due to evaporation, the solution was frequently replenished in order to maintain the level to one-third of the height of cylinders. Also, the solution was replaced with a fresh one every 30 cycles (days).

Concrete cylinders were visually monitored for up to four months of PSA exposure. Moreover, the variation of mass of specimens with respect to the initial mass was calculated every 15 days of exposure according to:

$$\text{Mass loss at (t)} = (M_i - M_t) / M_i \times 100 \quad (1)$$

where t is the time, M_i is the initial mass of the coated cylinder; M_t is the mass of the cylinder at time t.

To investigate the effect of efficiency of coatings at mitigating the degradation of concrete surface induced by PSA, scanning electron microscopy (SEM) assisted with energy-dispersive X-ray analysis (EDX) was applied on fracture surfaces of specimens. The fracture pieces selected for the SEM analysis were extracted from the reaction front (surface of the specimens) and were coated with a fine layer of carbon before performing the analysis to make the surface conductive and to improve sample imaging. Moreover, mineralogical and thermal studies were conducted using differential scanning calorimetry (DSC) on powder samples extracted from the surface or core of selected specimens exposed to the solutions. The powder samples were prepared from extracted fracture pieces of specimens, which were pulverized to fine powder passing through sieve #200 (75 µm).

4.0 RESULTS

4.1 Visual Assessment

Concrete cylinders were continuously monitored during the PSA exposure. After three cycles, salt crystals started to deposit on the evaporative surface of untreated specimens due to the high rate of solution supply by capillary suction in concrete with w/b of 0.6 relative to the evaporation rate determined by the ambient conditions. With PSA cycling, efflorescence notably accumulated on the drying surfaces, followed by surface scaling and flaking. Fig. 1 shows the development of damage over time for untreated specimens (observations were made every 15 cycles). During the first 15 cycles, surface scaling initiated just above the solution level in the container (50 mm) and gravel started to appear; subsequently, scaling rapidly propagated upwards to reach the top of specimens after 45 cycles of exposure, while the immersed part remained intact. After 60 cycles, the cross section of the upper part was reduced significantly accompanied by notable loss of paste and debonding of aggregate. Untreated specimens failed after 105 cycles before the proposed period of exposure (120 cycles).

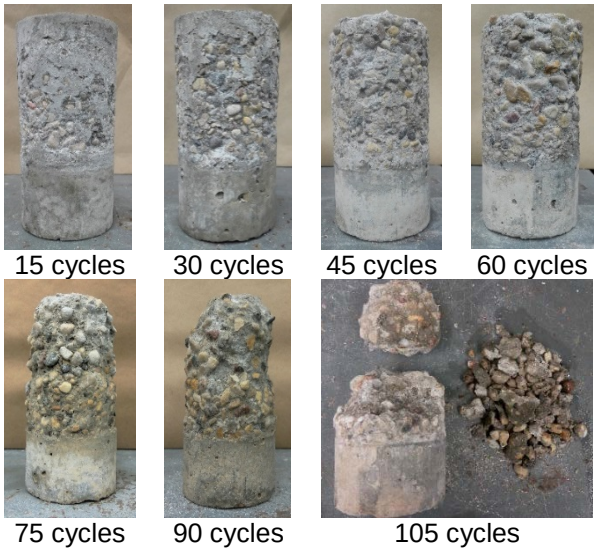

Fig. 1. Sequence of degradation of untreated specimens at different ages of exposure

Figure 2 shows the coated concrete after 120 cycles of exposure. As shown, epoxy coated cylinders did not show any signs of deterioration and the coating

remained intact till the end of test. Regarding other types of treatment, ethyl silicate was effective to a great extent in minimizing the surface damage; only minor scaling occurred within 20 mm above the sodium sulfate level. On the other hand, silane treated samples fractured after 120 cycles of PSA regime.

(a) (b) (c)

Fig. 2. State of coated specimens after 120 days of PSA exposure: (a) epoxy, (b) silane, and (c) ethyl silicate, respectively

4.2 Mass Change

The mass change of concrete specimens (uncoated and coated) was determined every 15 cycles as shown in Fig. 3. Complying with the visual inspection results, uncoated specimens experienced mass loss after 15 cycles. The rate of loss was low up to 60 days, and it substantially increased afterwards till failure. Coated specimens showed a slight mass increase at the beginning of exposure which could be attributed to the ingress of salt solution into the bottom part of concrete. This trend was not observed for uncoated specimens as the mass loss caused by PSA was higher than gain due to solution absorption.

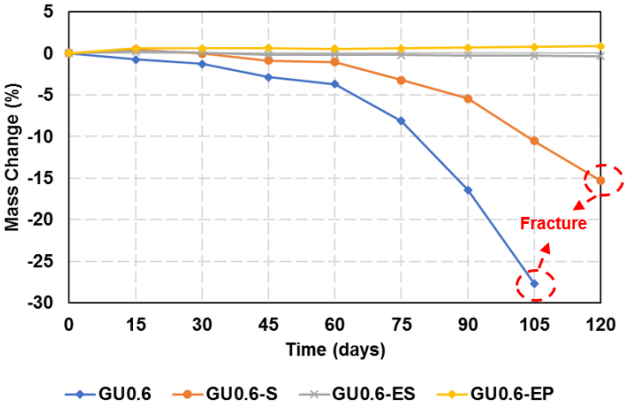

Fig. 3. Average mass change of untreated and treated specimens throughout the exposure

The effect of coatings on mass change behaviour differed. For instance, silane treated samples showed similar degradation pattern to uncoated concrete. However, the rate of mass loss was notably slower than that of uncoated specimens with a maximum mass loss of 10% at 105 days; however, these specimens fractured at the end of testing. On contrary, cylinders coated with ethyl silicate showed a negligible rate of damage and the loss of specimens was almost unchanged. Concrete specimens coated with epoxy increased slightly in mass throughout the exposure due to salt uptake and at the same time, no scaling was occurring.

5.0 DISCUSSION

5.1 Mechanism of Damage

Untreated specimens underwent severe mass loss from the upper portion exposed to cyclic temperature and humidity while the lower portion remained intact. The short period of chemical exposure in the immersed portion was insufficient for the inducing external sulfate attack to a damaging level. This is substantiated by the absence of damage manifestations in this part and limited occurrence of sulfate reaction products as shown by the SEM and DSC analyses of the surface layer below solution level (Figs. 4 and 5).

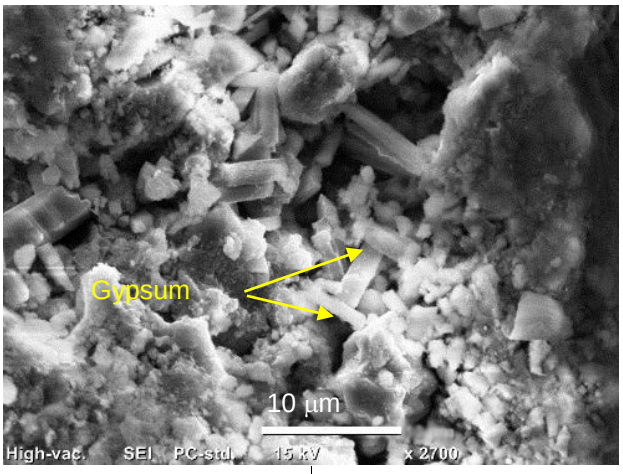

Fig. 4. SEM of surface layer of uncoated specimens immersed in sodium sulfate showing gypsum crystallites.

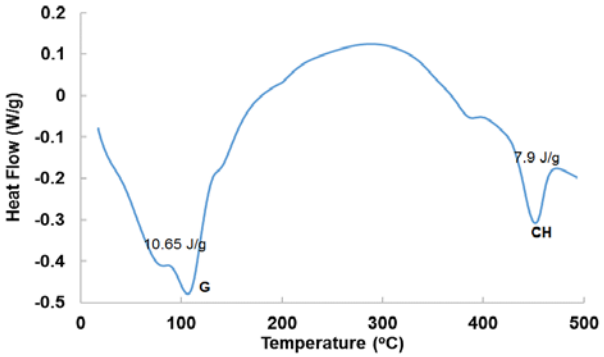

Fig. 5. DSC on samples extracted from the immersed part of uncoated samples (G = gypsum; CH = calcium hydroxide)

The main reason for damage uncoated specimens was the formation of sub-efflorescence depositing

beneath the surface that caused considerable pressure on concrete, and subsequently scaling and flaking as shown in Fig. 6. Sub-efflorescence forms due to capillary rise of sodium sulfate through concrete with a rate slower than evaporation rate due to ambient conditions. SEM and EDX analyses on the scaled layers showed the existence of massively stacked planes of sodium sulfate (Fig. 7)

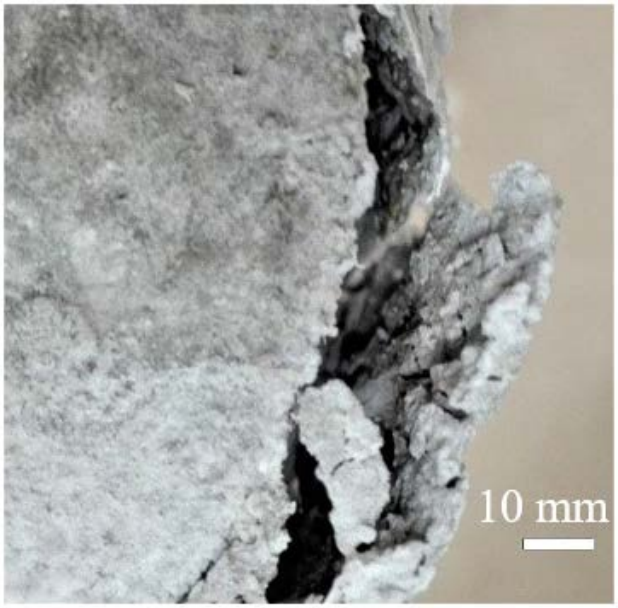

Fig. 6. Spalling of surface concrete due to formation of sub-efflorescence

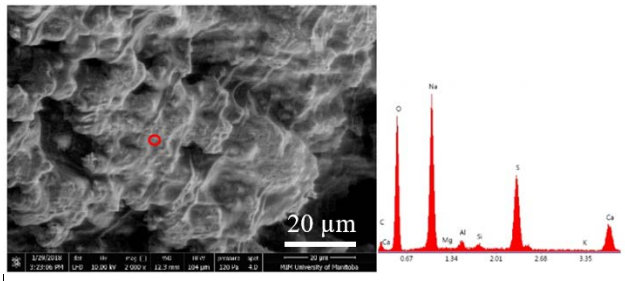

Fig. 7. SEM and EDX of the scaled surface layer of uncoated specimens above the solution level

Indeed, the high rate of damage can be attributed to the increased porosity of concrete made with w/b of 0.60. The high penetrability of concrete (i.e. increased total volume of pores and enhanced connectivity) led to fast capillary rise and rapid rate of solution uptake which caused large amounts of salt to crystallize within the surface pores and consequently increased surface scaling. This trend agrees with the effect of w/b on concrete damage by PSA (Bassuoni and Rahman, 2016; Lee and Kurtis, 2017). Moreover, conversion between thenardite (forms during drying stage of test) and mirabilite (forms during wetting stage of test) aided in the accelerated progression of damage since transformation between these phases may result in higher super saturation ratio and damage, as given by Corren's (1949) model of crystallization pressure:

$$P = \frac{RT}{V}\ln\left(\frac{C}{Cs}\right) \quad (2)$$

where, P is the crystallization pressure, R is the ideal gas constant, T is the temperature, V is the molar volume of the solid salt, C is the concentration of the solution, C_s is saturation concentration of the solution and C/C_s is the supersaturation ratio.

5.2 Surface Coatings

Epoxy is a common surface coating applied for concrete protection. It forms a continuous and thick polymer surface that provides a physical barrier against detrimental substances from the surrounding environment; accordingly, it may enhance concrete durability. In this study, it was found that epoxy was successful in protecting concrete from PSA damage (Figs. 2 and 3), similar to findings of Suleiman *et al.* (2014). The SEM and EDX analyses (Fig. 8) showed absence of salt depositions in the pores at the interface between epoxy and concrete. This indicated minimal capillary rise of salt solution within the interface layer between epoxy and substrate concrete. Also, epoxy might prevent the evaporation of salt solution diffused upwards through the concrete core. In addition, the high tensile strength of epoxy (44 MPa) may resist salt crystallization pressures, if any. Some traces of gypsum were found by DSC analysis as shown in Fig. 9.

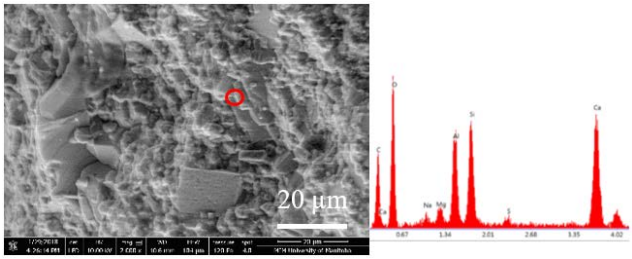

Fig. 8. SEM and EDX of surface layer beneath epoxy coating

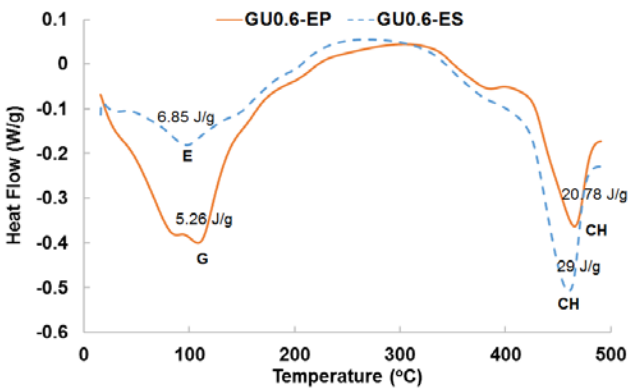

Fig. 9. DSC on samples extracted from concrete beneath the epoxy and ethyl silicate layers (E=ettringite; G=gypsum; CH=calcium hydroxide)

Silane is a hydrophobic agent that is characterized by small particle size allowing deep penetration into

concrete. It reacts with water in capillary pores to produce components capable of repelling diffusing ions as the contact angle of ions with surface becomes larger than 90° (Dai *et al.*, 2010). In this study, the recorded mass loss of concrete treated with silane was lower than those of uncoated specimens. However, silane was ineffective at mitigating PSA damage. This contradicts the conclusion of the previous study by Suleiman *et al.* (2014) in which silane was found effective in resisting PSA. This could be linked to the mild exposure conditions of PSA testing that were not sufficiently severe to evaluate silane performance. It was noticed that in the case of silane, scaling did not progress from the surface inwards. Instead, minor scaling was observed on the outer concrete and it proceeded very slowly till 60 cycles. Then, map cracking appeared on the surface, which led to peeling of a surface concrete layer having around 2-3 mm thickness. Once this layer was detached, scaling proceeded at a very rapid rate similar to uncoated specimens (Fig. 10). The microscopy analysis of the inner face of the layer showed that massive planes of sodium sulfate crystals existed beneath the surface (Fig. 11).

Fig. 10. Map cracking and detachment of a surface layer from silane treated concrete cylinders

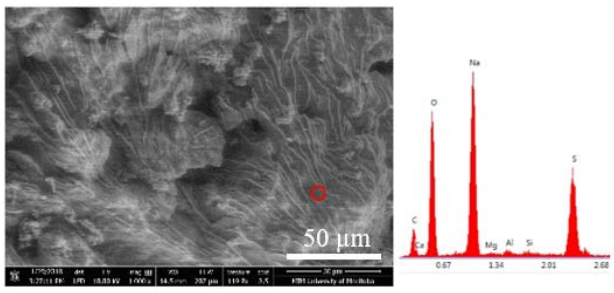

Fig. 11. SEM and EDX of detached surface layer from silane coated samples

This might suggest that the mechanism of damage in this case was according to the following sequence; initially, hydrophobic action of silane was effective at preventing capillary rise onto the concrete surface leading to insignificant crystallization and scaling. Subsequently, continuous uptake of solution though the bottom concrete core and salt crystallization beneath the silane layer caused built-up of pressure that pushed against the surface layers causing its detachment. However, interesting results were obtained through the microscopy analysis indicating that the damage in this case was a combined action between physical and chemical sulfate attack. Analysis on fracture pieces of concrete immediately below the scaled layer showed the existence of sodium sulfate on the edge; proceeding inwards, a zone of combined ettringite and sodium sulfate was found followed by a zone full of ettringite (Fig. 12). Figure 13 shows SEM images and EDX results from each of these zones.

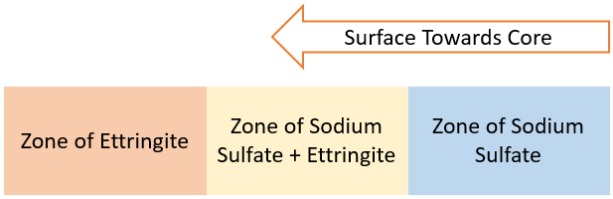

Fig. 12. Formed compounds below-detached layer concrete in silane-treated samples

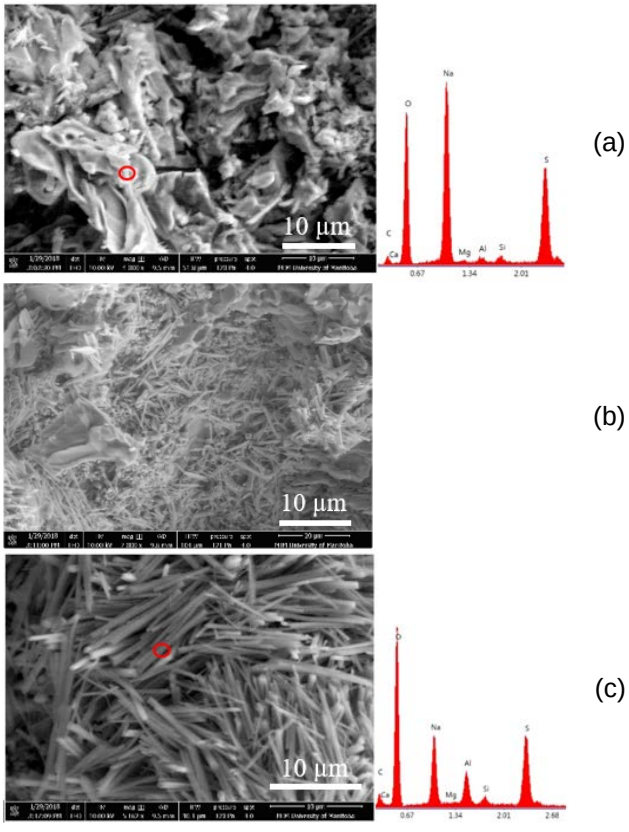

Fig. 13. Formed compounds below-detached layer in silane-treated samples: (a) sodium sulfate, (b) sodium sulfate + ettringite and (c) ettringite

Analysis was supported by DSC results (shown in Fig. 14) which showed the formation of sodium sulfate in the extracted sample from scaled layer with no traces for ettringite. On contrary, core samples showed excessive formation of ettringite with minor peak of sodium sulfate.

In comparison, the DSC curve of samples obtained from upper portions of uncoated specimens (Fig. 14) shows similar features as silane; however, the amount of formed ettringite indicated by enthalpy was less by approximately 72%. Moreover, the amount of sodium sulfate was higher for the uncoated specimens. It is proposed that the lower rate of evaporation through silane led to slow surface scaling progression (Fig. 3), while at the same time, ettringite was forming beneath the layer with massive amounts that caused excessive pressures caused the map cracking shown in Fig. 10 which is a symptom of chemical sulfate attack. Upon the peeling of this crust comprising silane (at around 75 cycles), the surface scaling progressed rapidly due to PSA until fracture. This pattern of cracking and subsequent scaling did not appear in the uncoated specimens since the surface scaling progressed rapidly from the surface inwards indicating that although, chemical sulfate attack products formed, the main cause of damage was due to PSA.

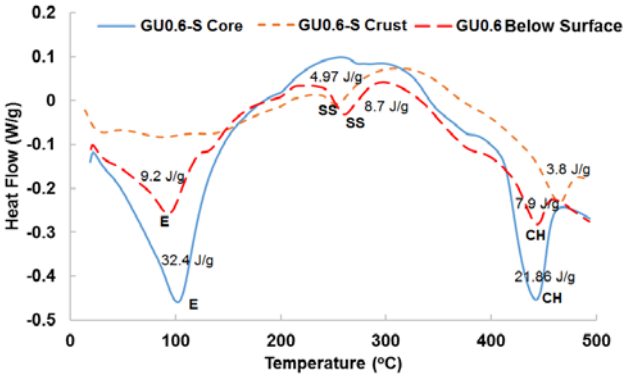

Fig. 14. DSC on samples extracted from scaled layer and core of silane coated samples and from upper portion of uncoated samples (E = ettringite; SS = sodium sulfate; CH = calcium hydroxide)

The application of ethyl silicate to concrete led to a satisfactory performance under this PSA exposure. It has dual functions: pore-blocking and water-repelling. Silicates can react with calcium hydroxide resulting in silica gel that acts as a micro-filler, generating a compact microstructure and dense surface layer. Furthermore, its low viscosity and small molecular size permit it to diffuse inside concrete. It was reported that ethyl silicate is effective at decreasing water absorption and vapour transmission coefficient due to densified superficial pore structure originating from its pozzolanic reactivity and filler effect in the surface pores (Hou *et al.*, 2014; 2015). The SEM analysis of the surface layer did not show any feature of damage (Fig. 15); however, some traces of ettringite was founded in the samples away from the surface, which was also supported by thermal analysis (Fig. 9).

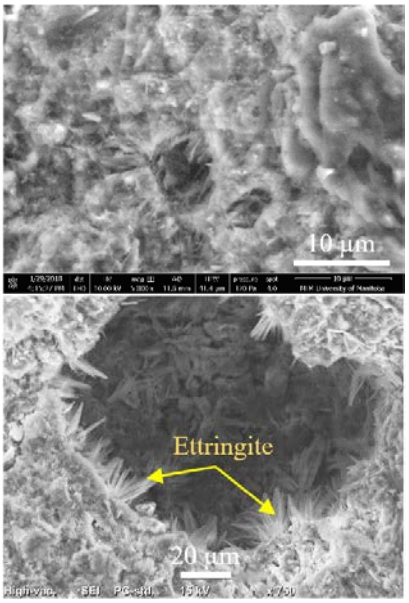

(a)

(b)

Fig. 15. SEM of (a) surface and (b) inner parts of ethyl silicate coated specimens

It was noticed that the enthalpy of ettringite in case of ethyl silicate (6.85 J/g) is similar to that of gypsum in case of epoxy (5.26 J/g) indicting proportionate levels of chemical sulfate attack. This suggests that limited evaporation (caused by both materials) helped to minimize damage unlike the case of silane which permitted higher rate of evaporation/wicking.

6.0 CONCLUSIONS

In this study, three coatings performing different functions were tested for protecting concrete against physical salt attack (PSA). Based on the previous discussion, the following conclusions can be made:

- Untreated concrete made with high w/b (e.g. 0.6) was highly susceptible to damage when partially immersed in sodium sulfate solution. Moreover, the selected regime for testing was suitable to give reliable trends of concrete performance under PSA.
- Epoxy and ethyl silicate were effective at minimizing/eliminating the damage caused by PSA due to their membrane action and pore blocking and hydrophobic action, respectively.
- Silane was not appropriate to be applied in case of PSA as samples were fractured before end of testing; although silane specimens did not initially show excessive scaling due to PSA, surface cracking and expansion caused by ettringite, together with PSA at the surface led to fracture of specimens at 120 cycles.

- For the test mixture, damage generally occurred due to combined action of physical and chemical sulfate attacks. However, for uncoated specimens, deterioration mainly took place due to PSA unlike silane where chemical attack contributed significantly to damage.
- The rate of evaporation might influence which aspect of damage could prevail such that higher rate increases the possibility of physical damage rather than the chemical one.

Acknowledgement

The authors highly appreciate the sponsorship by Natural Sciences and Engineering Research Council of Canada (NSERC) and University of Manitoba Graduate Fellowship (UMGF). The IKO Construction Materials Testing Facility at the University of Manitoba in which these experiments were conducted has been instrumental to this research.

References

ASTM C192, 2016. Standard practice for making and curing concrete test specimens in the laboratory, ASTM International, West Conshohocken, PA, V. 4.02.

Barberena-Fernández, A. M., Carmona-Quiroga, P. M., Blanco-Varela, M. T., 2015. Interaction of TEOS with cementitious materials: chemical and physical effects. Cement and Concrete Composites. 55:145-152.

Bassuoni, M. T., Rahman, M. M., 2016. Response of concrete to accelerated physical salt attack exposure. Cement and Concrete Research, 79:395–408.

Correns, C.W., 1949. Growth and dissolution of crystals under linear pressure. Discussions of the Faraday Society, 5:267–271.

CSA A3001, 2013. Cementitious materials compendium, Canadian Standards Association, Toronto, Ontario, CA.

Dai, J. G., Akira, Y., Wittmann, F. H., Yokota, H., Zhang, P., 2010. Water repellent surface impregnation for extension of service life of reinforced concrete structures in marine environments: the role of cracks. Cement and Concrete Composites, 32(2):101-109.

Flatt, R. J., 2002. Salt damage in porous materials: how high supersaturations are generated. Journal of Crystal Growth, 242(3–4):435–454.

Folliard K. J., Sandberg, P., 1994. Mechanisms of concrete deterioration by sodium sulfate crystallization. ACI; SP145:933–945.

Haynes, H., Bassuoni, M. T., 2011. Physical Salt Attack on Concrete. Concrete International, 33(11):38-42.

Haynes, H., O'Neill, R., Mehta, P. K., 1996. Concrete deterioration from physical attack by salts. Concrete International, 18(1):63–68.

Haynes, H., O'Neill, R., Neff, M., Mehta, P. K., 2008. Salt weathering distress on concrete exposed to sodium sulfate environment. ACI Materials Journal, 105(1):35–43.

Hou, P., Cheng, X., Qian, J., Shah, S. P., 2014. Effects and mechanisms of surface treatment of hardened cement-based materials with colloidal nanoSiO2 and its precursor. Construction and Building Materials, 53:66-73.

Hou, P., Cheng, X., Qian, J., Zhang, R., Cao, W., Shah, S. P., 2015. Characteristics of surface-treatment of nano-SiO2 on the transport properties of hardened cement pastes with different water-to-cement ratios. Cement and Concrete Composites, 55:26-33.

Lee, B. Y., Kurtis, K. E., 2017. Effect of pore structure on salt crystallization damage of cement-based materials: Consideration of w/b and nanoparticle use. Cement and Concrete Research, 98:61-70.

Liu, Z., Zhang, F., Deng, D., Xie, Y., Long, G., Tang, X., 2017. Physical sulfate attack on concrete lining–A field case analysis. Case Studies in Construction Materials, 6:206-212.

Nehdi, M. L., Suleiman, A. R., Soliman, A. M., 2014. Investigation of concrete exposed to dual sulfate attack. Cement and Concrete Research, 64:42–53.

Rodriguez-Navarro, C., Doehne, E., 1999. Salt weathering: influence of evaporation rate, supersaturation and crystallization pattern. Earth Surf Process Landforms, 24(2-3):191–209.

Stark, D., 1989. Durability of concrete in sulfate-rich soils. RD O97, Portland Cement Association, Skokie, Illinois.

Stark, D., 2002. Performance of concrete in sulfate environments. RD129, Portland Cement Association, Skokie, Illinois.

Suleiman, A. R., Soliman, A. M., Nehdi, M. L., 2014. Effect of surface treatment materials on durability of concrete exposed to physical sulfate attack. Constructions and Building Materials, 73:674–681.

Woo, R. S., Zhu, H., Chow, M. M., Leung, C. K., Kim, J., 2008. Barrier performance of silane–clay nanocomposite coatings on concrete structure. Composites Science and Technology. 68 (14):2828-2836.

Yoshida, N., Matsunami, Y., Nagayama, M., Sakai, E., 2010. Salt weathering in residential concrete foundations exposed to sulfate-bearing ground. Journal of Advanced Concrete Technology, 8(2):121-134.

Zhutovsky, S., Hooton, R. D., 2017. Experimental study on physical sulfate salt attack. Materials and Structures, 50-54.